Int. J. Heat Mass Transfer. Vol. 30, No. 7, pp. 1381–1389, 1987
Printed in Great Britain

0017–9310/87 \$3.00+0.00

Natural convection in uniformly heated vertical annuli

M. AL-ARABI, M. A. I. EL-SHAARAWI and M. KHAMIS
Mechanical Engineering Department, Alazhar University, Nasr City, Cairo, Egypt

(*Received* 7 *July* 1986)

Abstract—A numerical study of natural convection through vertical annuli with one wall uniformly heated and the other wall adiabatic was made. In this study the boundary layer simplifications of the Navier–Stokes equations for developing laminar flow with constant properties were solved by means of a finite-difference method. Three radius ratios (0.26, 0.5 and 0.9) were investigated. The different variables (velocity, pressure defect, temperature, etc.) were determined. An apparatus was built to check the obtained numerical results for one of the conditions employed. Agreement between the theoretical and experimental values was good.

INTRODUCTION

CONSIDERABLE interest has been shown in recent years in the problem of natural convection heat transfer to fluids in heated, vertical, open-ended annuli. Such systems are of practical importance in the field of double pipe arrangements particularly the fuel elements of nuclear reactors during shut-off periods. They may also be useful in solar heating and ventilating applications for domestic purposes.

To the authors' knowledge, the only study available at present for natural convection heat transfer in vertical annuli is that of El-Shaarawi and Sarhan [1]. They presented numerical results for the problem of laminar, natural convection heat transfer in an open-ended vertical concentric annulus of radius ratio 0.5 with one wall isothermal and the other wall adiabatic. Apart from this work the data available in the literature on heat transfer in annuli are for either forced flow or mixed convection [3]. On the other hand, natural convection heat transfer in tubes and parallel plate channels, which are the two limits of the annular geometry, have received most attention [4–8].

The lack of information on natural convection heat transfer in vertical annuli with constant wall heat flux motivated the present work. This paper presents numerical and experimental results for natural convection heat transfer in vertical annuli with one wall heated at constant heat flux while the other wall is adiabatic. In the numerical analysis, the governing boundary layer equations have been solved with Prandtl number = 0.7 for annuli of radius ratios 0.26, 0.5, and 0.9 under two thermal boundary conditions; namely, case (I) in which the inner wall of the annulus is uniformly heated while the outer wall is adiabatic and case (O) in which the outer wall is uniformly heated while the inner wall is adiabatic. In the experiments, measurements were made using a specially constructed apparatus with an annulus of radius ratio equal to 0.26 under thermal boundary condition (O). A comparison between the theoretical results and the experimental measurements for this radius ratio is presented.

THEORETICAL ANALYSIS AND METHOD OF SOLUTION

The geometry of the problem under consideration and the coordinate system used are illustrated in Fig. 1. Either the inner or outer wall of the annulus is uniformly heated while the other wall is perfectly insulated. The heat added to one of the annulus boundaries produces an upward natural convection flow in the annular gap between the two cylindrical walls. It is assumed that the fluid enters the bottom of the annulus with a flat velocity profile at a value equal to the mean axial velocity in the annular gap (u_0) and with a uniform temperature profile at a value equal to the ambient temperature (t_0). The fluid is assumed to have constant physical properties but obeys the Boussinesq approximation, according to which its density is constant except in the buoyancy term of the vertical momentum equation. The flow is steady, axisymmetric and without internal heat generation. Viscous dissipation and axial diffusion of heat are neglected. Further, applying the Prandtl boundary layer assumptions, the radial momentum equation can be dropped, the axial diffusion of momentum can be neglected, and the equations governing the natural convection laminar fluid motion and heat transfer in the gap of the vertical concentric annulus are

$$\frac{\partial v}{\partial r}+\frac{v}{r}+\frac{\partial u}{\partial z}=0 \qquad (1)$$

NOMENCLATURE

a	local heat transfer coefficient based on area of heated surface, $q/(t_w - t_m)$
$\bar{a}$	average heat transfer coefficient over the annulus height based on average temperature of heated wall, $\bar{h}/\pi D_w l(\bar{t}_w - t_0)$
b	annular gap width, $(r_2 - r_1)$
c_p	specific heat of fluid at constant pressure
D	equivalent (hydraulic) diameter of annulus, $2b$
D_w	diameter of heated wall
f	volumetric flow rate, $\int_{r_1}^{r_2} 2\pi r u \, dr = \pi(r_2^2 - r_1^2)u_0$
F	dimensionless volumetric flow rate, $f/\pi l Gr^* \nu$
g	gravitational body force per unit mass
Gr	Grashof number, $g\beta q D^4/2\nu^2 k$
Gr^*	modified Grashof number, $Gr\, D/l$
h	heat absorbed by fluid from entrance up to a particular elevation in the annulus, $\rho_0 f c_p(t_m - t_0)$
$\bar{h}$	heat absorbed by fluid from entrance up to the annulus exit, i.e. value of h at $z = l$, $\rho_0 c_p f(\bar{t}_m - t_0) = \pi D_w l q$
H	dimensionless heat absorbed from entrance up to a particular elevation, $2hk/\pi\rho_0 c_p \nu\, Gr^*\, qDl$
$\bar{H}$	dimensionless heat absorbed from entrance up to annulus exit, i.e. value of H at $z = l$, $2\bar{h}k/\pi\rho_0 c_p \nu\, Gr^*\, qDl$
k	thermal conductivity of fluid
l	height of annulus
L	dimensionless annulus height, $1/Gr^*$
N	annulus radius ratio, r_1/r_2
Nu	local Nusselt number, $aD/k = 2/(T_w - T_m)$
$\overline{Nu}$	average Nusselt number, $\bar{a}D/k = 2/\bar{T}_w$
p	pressure of fluid at any cross-section
p'	pressure defect at any cross-section, $p - p_s$
p_0	pressure of fluid at annulus entrance
p_s	hydrostatic pressure at any particular elevation, $-\rho_0 g z$
P	dimensionless pressure defect, $p' r_2^4/\rho_0 l^2 \nu^2 Gr^{*2}$
Pr	Prandtl number, $\mu c_p/k$
q	heat flux at heated wall, $\mp k(\partial t/\partial r)\vert_w$ where the minus and plus signs are for cases (I) and (O), respectively
r	radial coordinate
r_1	inner radius of annulus
r_2	outer radius of annulus
R	dimensionless radial coordinate, r/r_2
Ra	Rayleigh number, $Gr\, Pr$
Ra^*	modified Rayleigh number, $Gr^*\, Pr$
t	fluid temperature at any point
t_m	mixing cup temperature over any cross-section, $\int_{r_1}^{r_2} utr\, dr / \int_{r_1}^{r_2} ur\, dr$
$\bar{t}_m$	mixing cup temperature over the exit cross-section, i.e. value of t_m at $z = l$
t_0	fluid temperature at annulus entrance
t_w	temperature of heated wall at any particular elevation
$\bar{t}_w$	average temperature of heated wall, $(1/l)\int_0^l t_w\, dz$
T	dimensionless temperature at any point, $(t - t_0)/(qD/2k)$
T_m	dimensionless mixing cup temperature over any cross-section, $(t_m - t_0)/(qD/2k) = \int_N^1 UTR\, dR / \int_N^1 UR\, dR$
T_w	dimensionless temperature of heated wall at any particular elevation, $(t_w - t_0)/(qD/2k)$
$\bar{T}_w$	dimensionless average temperature of heated wall, $(\bar{t}_w - t_0)/(qD/2k) = (1/L)\int_0^L T_w\, dZ$
u	axial velocity component at any point
u_0	entrance axial velocity, $\int_{r_1}^{r_2} 2ur\, dr/(r_2^2 - r_1^2)$
U	dimensionless axial velocity component, $ur_2^2/l\nu\, Gr^*$
U_0	dimensionless axial velocity at annulus entrance, $u_0 r_2^2/l\nu\, Gr^*$
v	radial velocity component at any point
V	dimensionless radial velocity component, vr_2/ν
z	axial coordinate
Z	dimensionless axial coordinate $z/l\, Gr^*$.

Greek symbols

α	thermal diffusivity of fluid, $k/\rho_0 c_p$
β	volumetric coefficient of thermal expansion
μ	dynamic fluid viscosity
ν	kinematic fluid viscosity, μ/ρ_0
ρ	fluid density at temperature t, $\rho_0[1 - \beta(t - t_0)]$
ρ_0	fluid density at inlet fluid temperature
ϕ	dimensionless radial coordinate, $(r - r_1)/(r_2 - r_1)$.

$$\rho_0\left[v\frac{\partial u}{\partial r} + u\frac{\partial u}{\partial z}\right] = -\frac{\partial p}{\partial z} - \rho g + \frac{\mu}{r}\frac{\partial}{\partial r}\left(r\frac{\partial u}{\partial r}\right) \quad (2)$$

$$v\frac{\partial t}{\partial r} + u\frac{\partial t}{\partial z} = \frac{\alpha}{r}\frac{\partial}{\partial r}\left(r\frac{\partial t}{\partial r}\right). \quad (3)$$

Introducing the coefficient of thermal expansion (β) and the pressure defect (p') equation (2) can be written as

$$v\frac{\partial u}{\partial r} + u\frac{\partial u}{\partial z} = -\frac{1}{\rho_0}\frac{\partial p'}{\partial z} + g\beta(t - t_0) + \frac{\alpha}{r}\frac{\partial}{\partial r}\left(r\frac{\partial u}{\partial r}\right). \quad (4)$$

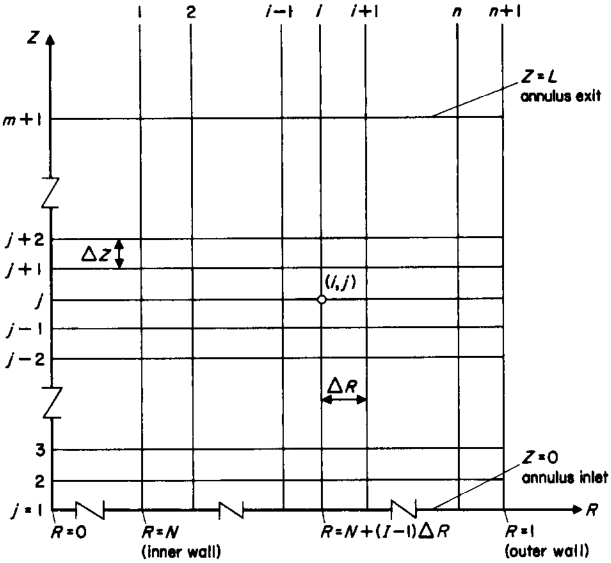

FIG. 1. Mesh network.

Equations (1), (3) and (4) are subject to the following boundary conditions:

$$\left.\begin{aligned}
&\text{for } z = 0 \text{ and } r_1 < r < r_2, v = 0, u = u_0,\\
&\qquad t = t_0 \text{ and } p' = p_0 = -\frac{\rho_0 u_0^2}{2}\\
&\text{for } z \geqslant 0 \text{ and } r = r_1, v = u = 0 \text{ and } \frac{\partial t}{\partial r} = -\frac{q}{k}\\
&\qquad \text{for case (I) or } \frac{\partial t}{\partial r} = 0 \text{ for case (O)}\\
&\text{for } z \geqslant 0 \text{ and } r = r_2, v = u = 0 \text{ and } \frac{\partial t}{\partial r} = 0\\
&\qquad \text{for case (I) or } \frac{\partial t}{\partial r} = \frac{q}{k} \text{ for case (O)}\\
&\text{for } z = 1, p' = 0.
\end{aligned}\right\} \quad (5)$$

Introducing the dimensionless parameters given in the Nomenclature, equations (1), (3) and (4) and boundary conditions (5) can be replaced by the following dimensionless forms:

$$\frac{\partial V}{\partial R} + \frac{V}{R} + \frac{\partial U}{\partial Z} = 0 \quad (6)$$

$$V\frac{\partial U}{\partial R} + U\frac{\partial U}{\partial Z} = -\frac{\partial P}{\partial Z} + \frac{T}{16(1-N)^4} + \frac{\partial^2 U}{\partial R^2} + \frac{1}{R}\frac{\partial U}{\partial R} \quad (7)$$

$$V\frac{\partial T}{\partial R} + U\frac{\partial T}{\partial Z} = \frac{1}{Pr}\left(\frac{\partial^2 T}{\partial R^2} + \frac{1}{R}\frac{\partial T}{\partial R}\right) \quad (8)$$

$$\left.\begin{aligned}
&\text{for } Z = 0 \text{ and } N < R < 1, V = 0, U = U_0,\\
&\qquad T = 0 \text{ and } P = P_0 = -\frac{U_0^2}{2}\\
&\text{for } Z \geqslant 0 \text{ and } R = N, V = U = 0 \text{ and } \frac{\partial T}{\partial R}\\
&\qquad = \frac{-1}{1-N} \text{ for case (I) or } \frac{\partial T}{\partial R} = 0 \text{ for case (O)}\\
&\text{for } Z \geqslant 0 \text{ and } R = 1, V = U = 0 \text{ and } \frac{\partial T}{\partial R} = 0\\
&\qquad \text{for case (I) or } \frac{\partial T}{\partial R} = \frac{1}{1-N} \text{ for case (O)}\\
&\text{for } Z = L, P = 0.
\end{aligned}\right\} \quad (9)$$

The above set of coupled dimensionless equations (6)–(8) subject to boundary conditions (9), have been solved by means of the linearized numerical scheme of Bodoia and Osterle [4] after replacing the derivatives in these equations by the appropriate finite-difference approximations given in ref. [9]. In this numerical technique, the mathematical need for another equation due to elimination of the radial momentum equation (as a result of the boundary layer simplifications) could be compensated, as explained by Coney and El-Shaarawi [2], by using the following dimensionless integral continuity equation:

$$F = (1-N^2)U_0 = 2\int_N^1 RU\,\mathrm{d}R. \quad (10)$$

It should be noted that in the present case of constant heat flux conditions there is no upper limiting value of F as in the case of constant wall temperature which was treated in ref. [1]. This is because under the constant heat flux condition the buoyancy driving force is sustained. The computations were carried out at various values of the dimensionless flow rate (F) ranging from 10^{-7} to 0.5 for each of the previously mentioned three radii ratios. For each value of F in an annulus of a given radius ratio (N), the computation starts at the bottom of the annulus and continues upward until the dimensionless pressure defect (P) ceases to be negative. The dimensionless axial distance (Z) from the annulus entrance until the cross-section at which $P = 0$ establishes the unknown dimensionless length (L) and hence the unknown modified Grashof number (Gr^*) for this particular value of F. Also, the computations give the dimensionless wall temperature T_w from which the average wall temperature $\bar{T}_w$ and hence the average Nusselt number $\overline{Nu}$ is evaluated.

The heat absorbed by the fluid from the entrance up to a particular elevation in the annulus is given by

$$h = c_p \rho_0 f(t_m - t_0) = 2\pi \rho_0 c_p \times \int_{r_1}^{r_2} ru(t - t_0)\,dr = \pi D_w zq \quad (11)$$

which can be written in the following dimensionless form:

$$H = \frac{2}{Pr\,Gr^*}\frac{h}{\pi Dlq} = \frac{2}{Pr}\frac{D_w}{D}Z = 2\int_N^1 RUT\,dR. \quad (12)$$

Hence

$$\bar{H} = \frac{2}{Pr}\frac{D_w}{D}L = \frac{2}{Ra^*}\frac{D_w}{D}. \quad (13)$$

Using equation (11), the following relation could be derived for the dimensionless mixing cup temperature

$$T_m = \frac{2}{Pr}\frac{D_w}{D}\frac{Z}{F}. \quad (14)$$

Equations (12) and (14) show that, for a given flow rate F of a specific fluid in a given annulus, the heat absorbed by the fluid (H) and the mixing cup temperature (T_m) vary linearly with Z.

APPARATUS

The experimental apparatus is shown diagrammatically in Fig. 2. It consists essentially of two

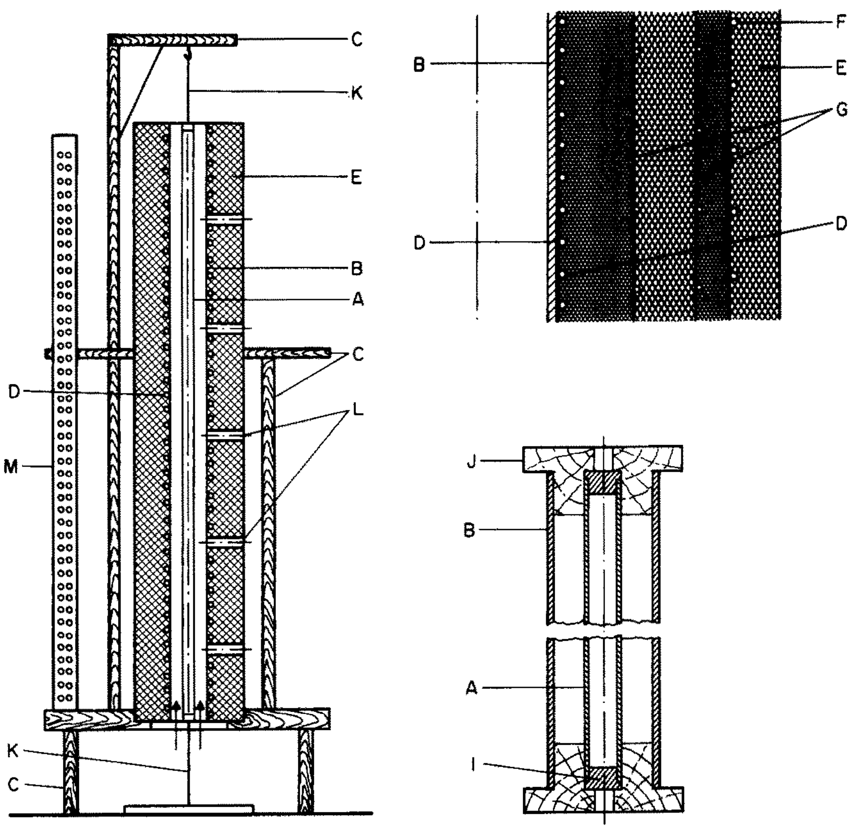

FIG. 2. Diagrammatic arrangement of the apparatus: (a) section in asbestos layers; (b) method of adjusting annulus concentrically. A, inner brass tube; B, outer copper tube; C, wooden frame; D, main heater; E, asbestos layers; F, guard heater; G, guard heater thermocouples; H, thermocouples; I, brass plugs; J, wooden guide; K, steel wires; L, measuring stations; M, wooden beam.

vertical concentric tubes forming a vertical annulus. The inner tube (A) is made of brass and has a 12.2 mm o.d., 10.1 mm i.d. and is 1670 mm long. The outer tube (B) is made of copper and has a 47 mm i.d., 51 mm o.d. and is also 1670 mm long. The annular radius ratio is 0.26, which is equal to one of the radius ratios investigated in the theoretical study. The whole apparatus is carried by means of a wooden frame (C).

The outer wall of the outer tube is covered with a layer of glass electric insulating tape on which a main heater (D) of nickel–chrome wire is uniformly wound in order to give a constant heat flux. The main heater is covered with asbestos layers (E) of thickness 55 mm, on which another nickel–chrome is uniformly wound to form a 'guard heater' (F) as shown in Fig. 2 (A). The guard heater is covered with a 15 mm thick asbestos layer. Four pairs of thermocouples (G) are installed at heights of 250, 550, 1050 and 1350 mm from the annulus entrance. The thermocouples of each pair are fitted on the same radius separated by a layer of asbestos. The heat generated by the guard heater can be adjusted, by means of a variable resistance, until the thermocouples of each pair read the same temperature. All the heat generated by the main heater then flows inwards to the annulus.

To measure the wall temperature of the outer tube 44 iron–constantan thermocouples (H) are silver-soldered along its outside surface. Counted from the annulus entrance the first ten thermocouples are located every 20 mm, the next 26 every 50 mm and the last eight every 20 mm. To make sure that heating is uniform circumferentially, eight thermocouples are fitted opposite to the main thermocouples at heights of 100, 300, 500, 700, 900, 1100, 1300 and 1500 mm from the annulus entrance. The thermocouples readings showed that heating was in all cases uniform along the circumference.

To obtain an adiabatic inner tube wall surface (i.e. boundary condition 'O'), the inner tube is filled with asbestos powder and the tube ends are closed by brass plugs (I). In order to set the tubes exactly concentric, two wooden guide pieces (J) were used (Fig. 2 (B)). Two steel wires (K) attached to the two end brass plugs fixed the inner tube to the wooden frame (C) carrying the apparatus.

Five measuring stations (L) are arranged on the outer tube at axial distances 200, 500, 800, 1100 and 1400 mm from the annulus entrance to enable measurement of the axial velocity and temperature profiles in the annular gap. Each station consists of a horizontal copper tube of 10 mm i.d. silver-soldered to the annular outer tube wall. When using one of the stations the four other stations are plugged. Screwed to the outer end of this tube is a travelling mechanism which carries either a Disa low-velocity hot-wire anemometer or a porcelain tube in which a travelling thermocouple is fitted. The thermocouple is shielded to minimize radiation. Calculation based on the outer tubes showed that radiation from the outer tube wall to the inner tube wall did not exceed 2.5% of the whole flux employed and radiation was, therefore, neglected.

The Disa low-velocity hot-wire anemometer was calibrated in the way recommended by the maker [10]. All the thermocouples used were calibrated against the melting point of ice made from distilled water and boiling points of several substances. A wooden beam (M) carried all the thermocouple wires on their way from the apparatus to a potentiometer capable of reading 0.0005 mV.

The required electric power was taken from the a.c. mains via a stabilizer. The main heater input was measured by a wattmeter accurate to $\pm 0.5\%$.

The apparatus was placed in a large room and a wooden shield, which extends well beyond the ends of the annulus, ensured no interference of outside air currents. All the readings were taken in the steady-state condition.

The experiments were carried out with heat flux values which ranged from 62 to 803 W giving modified Rayleigh number (Ra^*), volumetric air flow rate and maximum wall temperature in the range 2.27×10^4–2.92×10^5, 1400–2880 $cm^3\ s^{-1}$ and 100–600°C, respectively.

RESULTS AND DISCUSSION

For a complete set of results ref. [10] may be consulted. Only samples of these results are shown hereinafter.

Air velocity

Figures 3(a) and (b) show the theoretical profiles for the air velocity axial component corresponding to the two boundary conditions (O) and (I) in an annulus of $N = 0.26$ at the five heights corresponding to the five measuring stations of the experimental apparatus for values of $F = 1 \times 10^{-4}$ (low flux) and 5×10^{-5} (high flux).

It can be seen that the air velocity axial component profile is flat at the annulus entrance. As air flows up a boundary layer is formed at both annulus walls causing an unsymmetrical axial velocity profile with the peak shifted towards the heated wall. In view of continuity the value of the axial velocity on the outer side of the curve must correspondingly decrease until, as can be seen from Fig. 3(a), flow reversal occurs.

On the same figures the experimental points for boundary condition (O) are plotted. As can be seen the agreement with the theoretical curve is within $\pm 11\%$.

The theoretical air velocity radial component for a high and a low value of F is shown in Figs. 4(a) and (b), respectively. In the small flux condition the radial velocity is from both walls to the core whereas in the high flux condition the radial velocity is wholly towards the heated wall.

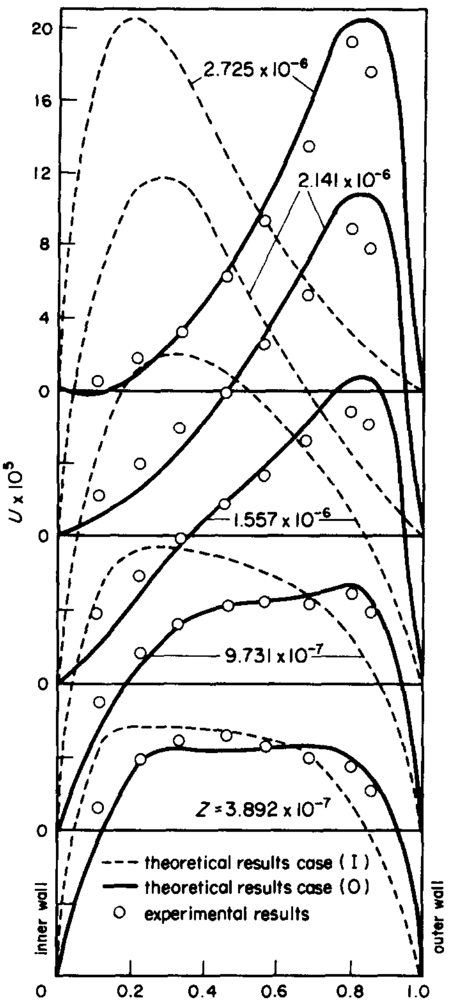

FIG. 3(a). Variation of axial velocity component: $N = 0.26$, $F = 1 \times 10^{-4}$, $q = 593$ W.

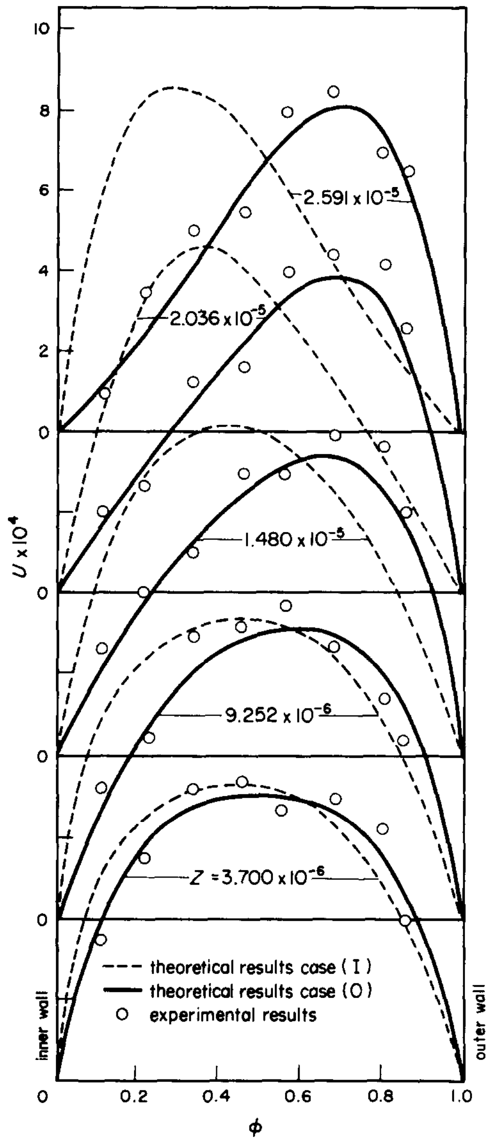

FIG. 3(b). Variation of axial velocity component: $N = 0.26$, $F = 5 \times 10^{-4}$, $q = 62$ W.

Air temperature

Figure 5 shows the theoretically obtained variation of air temperature radially for the two boundary conditions (O) and (I) in an annulus of $N = 0.26$ at the five heights Z corresponding to the five experimental measuring stations for a value of $F = 1 \times 10^{-4}$. It will be seen that the maximum temperature occurs at the heated wall and that the thickness of the boundary layer increases as the air moves up.

On the same figure the experimental points are plotted for boundary condition (O). Agreement with the theoretical curve is within $\pm 13\%$.

Wall and mixing cup temperature

The dimensionless temperature of the heated wall T_w and the dimensionless mixing cup temperature T_m are plotted in Fig. 6 against the dimensionless axial distance from the annulus entrance Z for the two boundary conditions (O) and (I) for an annulus of $N = 0.26$ and a value of $F = 1 \times 10^{-4}$.

The dimensionless mixing cup temperature is represented by a straight line (the flux along the annulus being constant). The dimensionless wall temperature curve, which shows a value of $T_w = 0$ at $Z = 0$ followed by a gradually rising value of $T_w - T_m$, indicates a developing region. At a value of $Z = \sim 1.75 \times 10^{-6}$ the fully developed condition appears to have been attained.

Plotted on the same figure are the experimental points for boundary condition (O) which agree with the theoretical curves within $\pm 9\%$ for T_w and within $\pm 6\%$ for T_m.

Local Nusselt number Nu

The values of the theoretical and the experimental local Nusselt number are also plotted in Fig. 6. The agreement is within $\pm 10\%$.

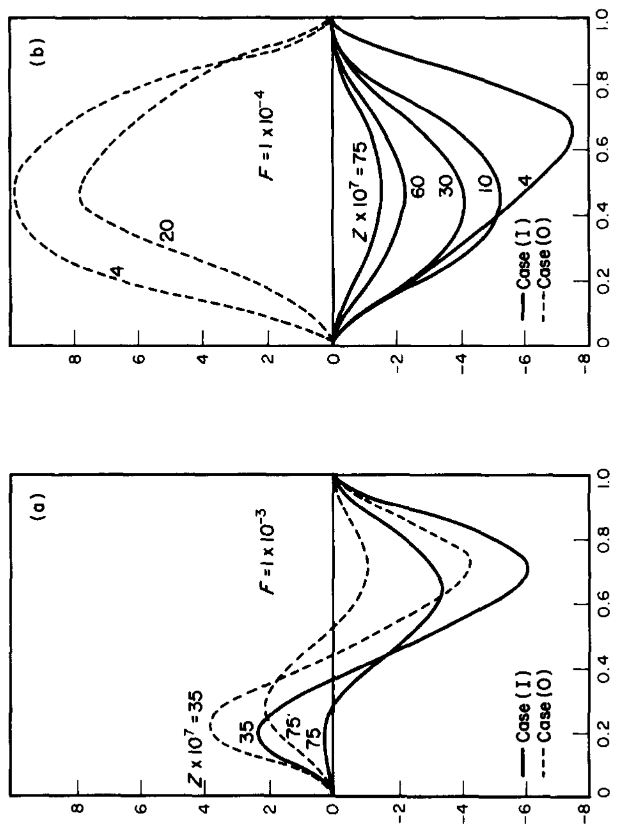

FIG. 4. Variation of radial velocity component: $N = 0.26$, $Pr = 0.7$.

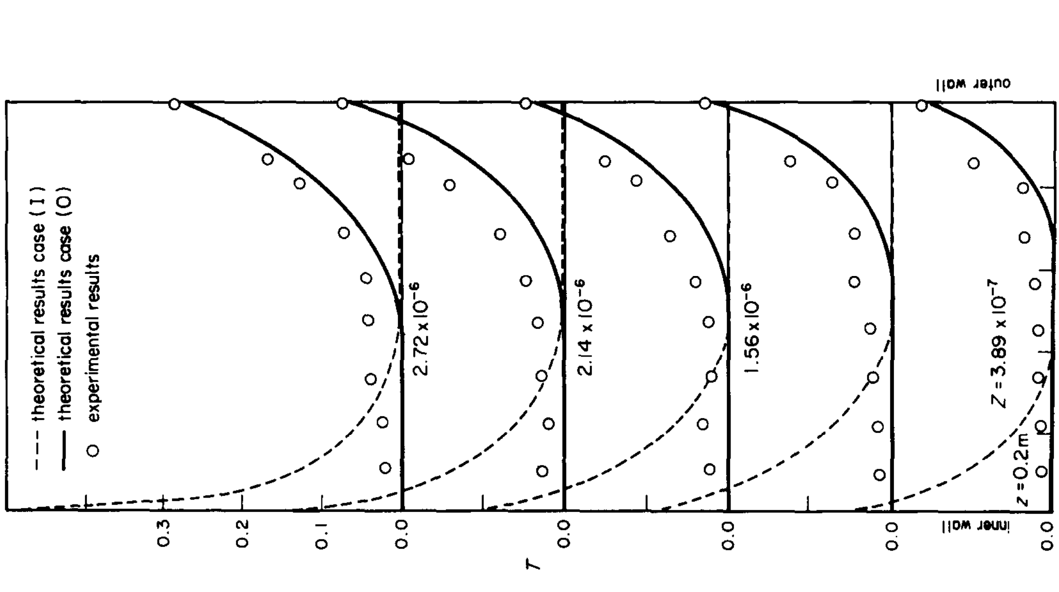

FIG. 5. Radial variation of temperature: $N = 0.26$, $F = 1 \times 10^{-4}$, $q = 593$ W.

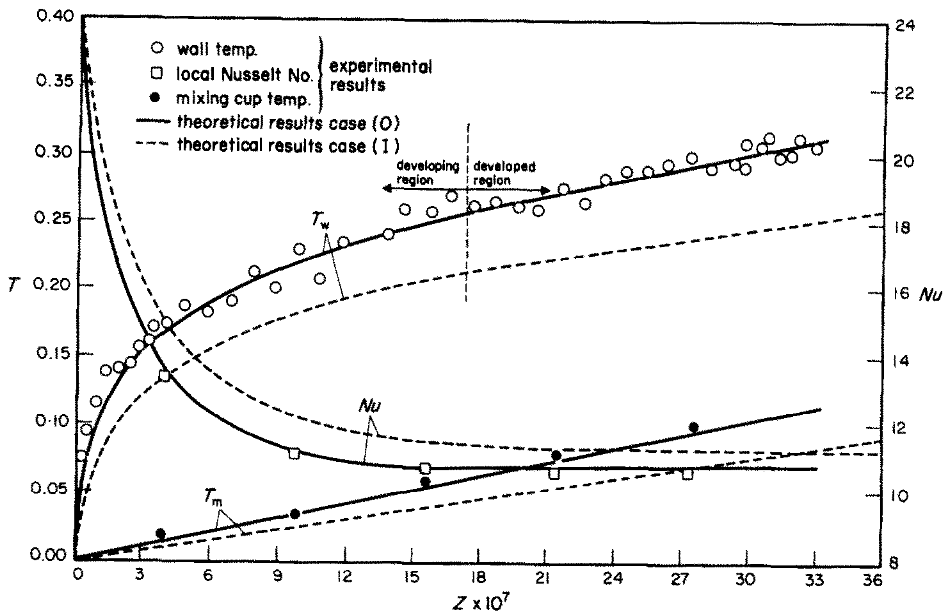

FIG. 6. Variation of Nu, T_w and T_m with Z: $Pr = 0.7$, $N = 0.26$, $F = 1 \times 10^{-4}$ and $q = 593$ W.

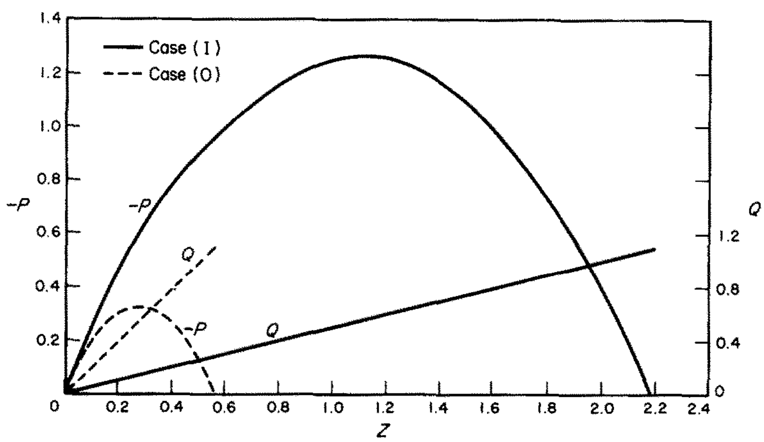

FIG. 7. Variation of pressure defect and heat absorbed with annulus length: $Pr = 0.7$, $N = 0.26$, $F = 1 \times 10^{-1}$.

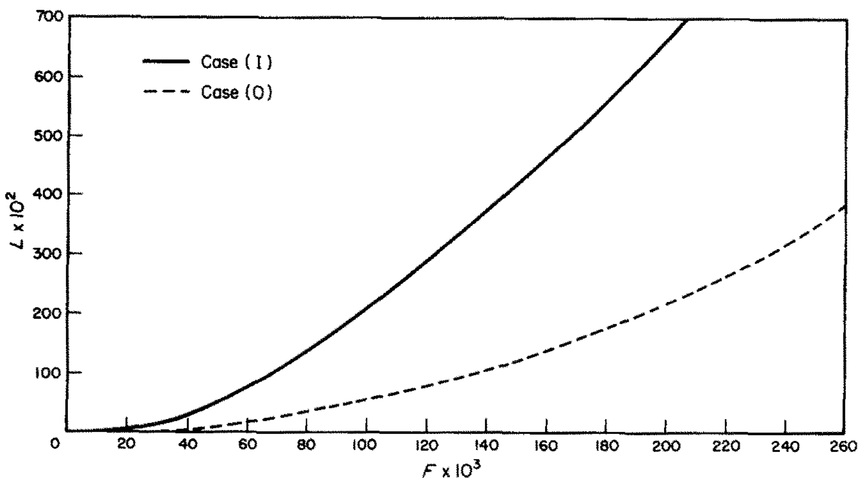

FIG. 8. Variation of dimensionless volumetric flow rate with the dimensionless annulus height: $Pr = 0.7$, $N = 0.26$.

Pressure defect

Figure 7 shows the variation of the dimensionless pressure defect P with the dimensionless axial distance Z for an annulus of $N = 0.26$ and a value of $F = 1 \times 10^{-1}$. It is to be noted that, in accordance with the definition given for the dimensionless annulus height L, the point of intersection of the P–Z curve with the Z-axis defines L.

It will be seen that the pressure defect starts with an initial value of $-\frac{1}{2}U_0^2$ and then decreases with Z until a minimum value is attained. It then increases again until it becomes equal to zero. This phenomenon may be explained by the fact that P is affected by two variables, the buoyancy force and the wall friction. In the 'entrance length' buoyancy is small compared with friction and as a result P decreases with Z. Then buoyancy increases until the axial distance $Z_{p_{\min}}$ becomes equal to the friction force. Beyond this point P increases until it becomes equal to zero at the annulus exit.

Relation between dimensionless annulus length L and dimensionless volumetric flow rate F

In practice it may be required to know the amount of air which flows through a certain annulus as a result of applying a certain flux when the pressure defect is zero at the annulus exit. The theoretical relation between L and F is drawn in Fig. 8 for an annulus of $N = 0.26$ and the two boundary conditions (O) and (I). It will be remembered that L is a function of the flux and that F is a function of the amount of air flowing.

REFERENCES

1. M. A. El-Shaarawi and A. Sarhan, Developing laminar free convection in a heated vertical open-ended annulus, *Ind. Engng Chem. Fundam.* **20,** 388–394 (1981).
2. J. E. R. Coney and M. A. I. El-Shaarawi, Finite difference analysis for laminar flow heat transfer in concentric annuli with simultaneously developing hydrodynamic and thermal boundary layers, *Int. J. Numer. Meth. Engng* **9,** 17–38 (1975).
3. M. A. I. El-Shaarawi and A. Sarhan, Free convection effects on the developing laminar flow in vertical concentric annuli, *J. Heat Transfer* **102,** 617–622 (1980).
4. J. R. Bodoia and F. Osterle, The development of free convection between heated vertical plates, *J. Heat Transfer* **84,** 40–44 (1962).
5. L. P. Davis and J. J. Perona, Development of free convection flow of a gas in a heated vertical open tube, *Int. J. Heat Mass Transfer* **14,** 889–903 (1971).
6. W. Aung, L. S. Fletcher and V. Sernas, Developing laminar free convection between vertical flat plates with asymmetric heating, *Int. J. Heat Mass Transfer* **15,** 2293–2308 (1972).
7. J. R. Dyer, The development of laminar natural convective flow in a vertical uniform heat flux duct, *Int. J. Heat Mass Transfer* **18,** 1455–1465 (1975).
8. J. R. Dyer, Natural convective flow through a vertical duct with a restriction entry, *Int. J. Heat Mass Transfer* **21,** 1341–1354 (1978).
9. M. A. I. El-Shaarawi and A. Sarhan, Developing laminar free convection in an open ended vertical annulus with a rotating inner cylinder, *J. Heat Transfer* **103,** 552–558 (1981).
10. M. Khamis, Experimental and theoretical study of laminar natural convection in an annulus, Ph.D. thesis, Mechanical Engineering Department, Alazhar University, Cairo, Egypt (1982).

CONVECTION NATURELLE DANS UN ESPACE ANNULAIRE VERTICAL UNIFORMEMENT CHAUFFE

Résumé—On étudie numériquement la convection naturelle dans un espace annulaire avec une paroi uniformément chauffée et l'autre adiabatique. Les simplications de la couche limite laminaire pour les équations de Navier–Stokes avec des propriétés constantes sont traitées par une méthode de différences finies. Trois rapports des rayons (0,26, 0,5 et 0,9) sont considérés. Les différentes variables (vitesse, pression, température, etc.) sont déterminées. Un montage est réalisé pour vérifier les résultats numériques obtenus pour une des conditions considérées. L'accord est bon entre les valeurs théoriques et expérimentales.

NATÜRLICHE KONVEKTION IN EINHEITLICH BEHEIZTEN SENKRECHTEN RINGRÄUMEN

Zusammenfassung—Es wurde eine numerische Untersuchung der natürlichen Konvektion in senkrechten Ringräumen, deren eine Wand adiabat ist und deren andere Wand einheitlich beheizt wird, durchgeführt. Mit Hilfe des Differenzenverfahrens wurden die Grenzschichtnäherungen der Navier–Stokes-Gleichungen für die laminare Anlaufströmung mit konstanten Stoffwerten gelöst. Drei Radienverhältnisse (0,26; 0,5 und 0,9) wurden untersucht. Verschiedene Größen (Geschwindigkeit, Druckverlust, Temperatur, etc.) wurden bestimmt. Um die numerischen Ergebnisse zu überprüfen, wurde eine der Anordnungen als Versuchseinrichtung realisiert. Die Übereinstimmung zwischen theoretischen und gemessenen Werten war gut.

ЕСТЕСТВЕННАЯ КОНВЕКЦИЯ В РАВНОМЕРНО НАГРЕВАЕМЫХ ВЕРТИКАЛЬНЫХ КОЛЬЦЕВЫХ КАНАЛАХ

Аннотация—Численно изучается естественная конвекция в вертикальном кольцевом канале, одна стенка которого равномерно нагревается, а другая—адиабатическая. В приближении пограничного слоя уравнения Навье–Стокса решались конечно-разностным методом для развивающегося ламинарного течения жидкости с постоянными свойствами. Исследовались три отношения радиусов 0,26, 0,5 и 0,9. Рассчитывались поля скоростей, давлений, температур. Создана установка для проверки полученных численных результатов для одного из заданных граничных условий. Получено хорошее согласие между теоретическими и экспериментальными результатами.